JOURNAL OF VIROLOGY, Aug. 2011, p. 8105–8115 Vol. 85, No. 16
0022-538X/11/$12.00 doi:10.1128/JVI.00735-11

A Recombinant Vesicular Stomatitis Virus Bearing a Lethal Mutation in the Glycoprotein Gene Uncovers a Second Site Suppressor That Restores Fusion▽

Megan L. Stanifer, David K. Cureton, and Sean P. J. Whelan*

Department of Microbiology and Molecular Genetics, Harvard Medical School, Boston, Massachusetts 02115

Received 12 April 2011/Accepted 1 June 2011

***Vesicular stomatitis virus* (VSV), a prototype of the *Rhabdoviridae* family, contains a single surface glycoprotein (G) that is responsible for attachment to cells and mediates membrane fusion. Working with the Indiana serotype of VSV, we employed a reverse genetic approach to produce fully authentic recombinant viral particles bearing lethal mutations in the G gene. By altering the hydrophobicity of the two fusion loops within G, we produced a panel of mutants, W72A, Y73A, Y116A, and A117F, that were nonfusogenic. Propagation of viruses bearing those lethal mutations in G completely depended on complementation by expression of the glycoprotein from the heterologous New Jersey serotype of VSV. The nonfusogenic G proteins oligomerize and are transported normally to the cell surface but fail to mediate acid pH-triggered membrane fusion. The nonfusogenic G proteins also interfered with the ability of wild-type G to mediate fusion, either by formation of mixed trimers or by inhibition of trimer function during fusion. Passage of one recombinant virus, A117F, identified a second site suppressor of the fusion block, E76K. When analyzed in the absence of the A117F substitution, E76K rendered G more sensitive to acid pH-triggered fusion, suggesting that this compensatory mutation is destabilizing. Our work provides a set of authentic recombinant VSV particles bearing lethal mutations in G, confirms that the hydrophobic fusion loops of VSV G protein are critical for membrane fusion, and underscores the importance of the sequence elements surrounding the hydrophobic tips of the fusion loops in driving fusion. This study has implications for understanding dominant targets for inhibition of G-mediated fusion. Moreover, the recombinant viral particles generated here will likely be useful in dissecting the mechanism of G-catalyzed fusion as well as study steps of viral assembly.**

Enveloped viral fusion machines fall into one of three classes: class I, II, or III. These classes are respectively exemplified by influenza A virus hemagglutinin (HA), flavivirus envelope (E) proteins, and the rhabdovirus glycoproteins (G) (18). All three classes of fusion proteins share basic characteristics. In response to specific triggers, conformational rearrangements in the protein lead to the insertion of a hydrophobic region(s) into the target cell membrane, followed by the refolding of the protein to bring the viral and cellular membrane in close proximity. Class I and II viral fusion machines undergo a priming cleavage event, and the conformational changes that occur on exposure to the appropriate trigger are irreversible. By contrast, the class III viral fusion machines do not undergo such a priming cleavage (as reviewed in reference 18). For rhabdoviruses, the trigger for conformational change in G is exposure to acidic pH. Uniquely, the pH-triggered conformational changes in class III fusion proteins are fully reversible, such that reexposure of viral particles to neutral pH results in G refolding into the prefusion conformation (4, 13, 31).

Vesicular stomatitis virus (VSV), the prototype of the *Rhabdoviridae* family, contains ≈400 trimeric spikes of G on its surface that mediate both attachment and fusion (41). VSV G can mediate attachment to and fusion with all eukaryotic cells in culture, suggesting that a cellular receptor is broadly distributed. Phosphatidylserine (PS) was thought to serve as a receptor for VSV, but reinvestigation of the role of PS in infection argued against its role as a receptor (5, 36). Recent work has also indicated that a client of the endoplasmic reticulum (ER) resident chaperone, GP96, may serve as the receptor molecule, since ablation of GP96 blocks VSV G-mediated attachment to cells (1). Attachment itself seems to be largely governed by electrostatic interactions through the net charge on the surface of G (5, 33). Following attachment, viral particles enter cells predominantly by an actin-dependent mode of clathrin-dependent endocytosis (6, 21, 40). Cellular uptake delivers the virus into the endosomal pathway, whereupon progressive acidification of the endosomal lumen and conformational changes in G mediate membrane fusion. In cell-cell and virus-cell fusion assays, the pH threshold at which G catalyzes fusion is 6.2 (27, 44), a finding that is consistent with the notion that viral particles can fuse from within an early endosomal compartment. Expression of a dominant negative version of Rab5, a GTPase that plays an important regulatory role in early endocytosis, inhibits VSV infection and suppresses particle uncoating, further suggesting that fusion occurs from an early endosomal compartment (28, 38). Evidence has, however, accumulated for an alternate two-step process of fusion in which the initial fusion event delivers the viral core into an intralumenal vesicle followed by a subsequent back-fusion event in which the contents of that vesicle are delivered into the cytoplasm from a late endosome (23). Irrespective of the pathway for delivery of the virus core, G-mediated membrane fusion is essential.

* Corresponding author. Mailing address: Department of Microbiology and Molecular Genetics, Harvard Medical School, 200 Longwood Ave., Boston, MA 02115. Phone: (617) 432-1923. Fax: (617) 738-7664. E-mail: swhelan@hms.harvard.edu.

▽ Published ahead of print on 15 June 2011.

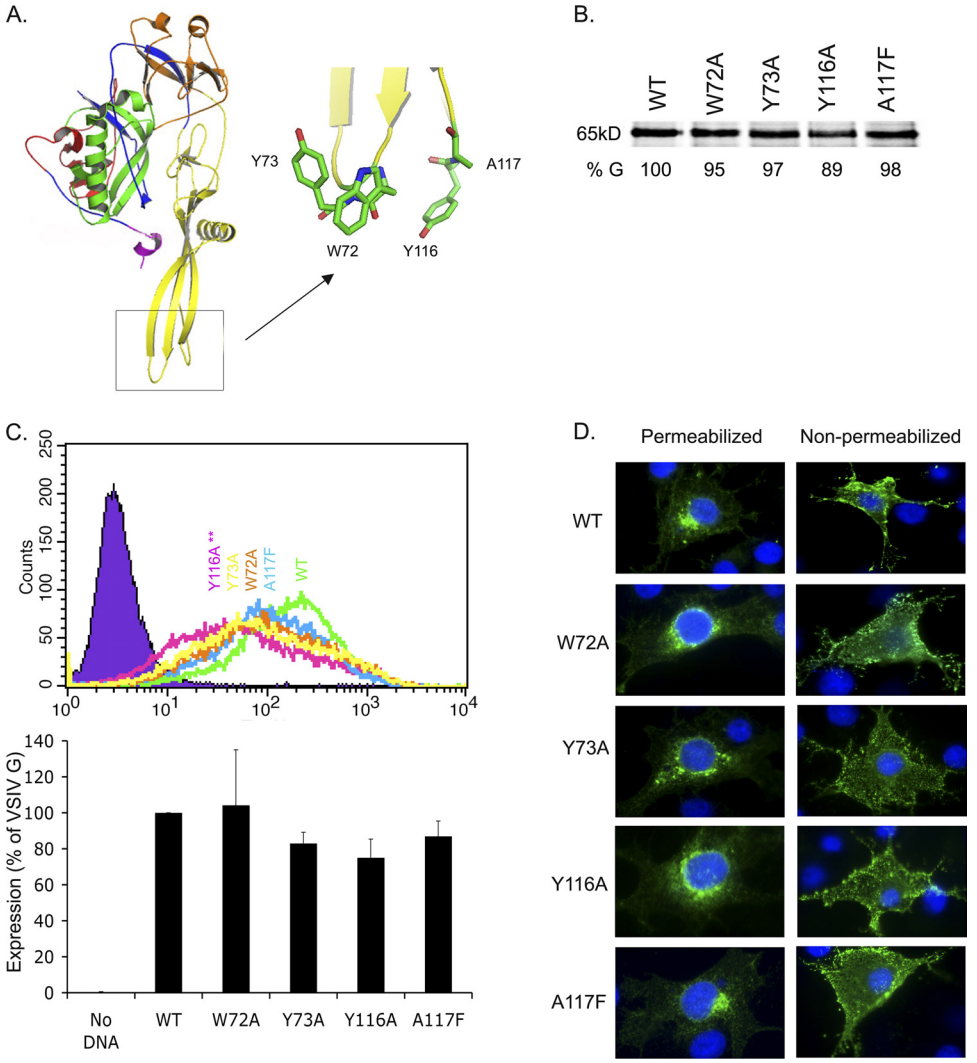

FIG. 1. Effects of modifications to the fusion loops on G expression and transport. (A) Structure of the prefusion form of VSIV G with an inset showing the two fusion loops. (B to D) BSR-T7 cells were infected with vTF7-3 at an MOI of 3 to 5 and subsequently transfected with 0.5 μg pGEM3 encoding the indicated VSIV G. (B) Total protein expression. Cells were pulsed with [^{35}S]Met-Cys 4.5 h posttransfection for 2 h. Cells were harvested, cytoplasmic extracts were prepared, and equal volumes of lysates were analyzed by electrophoresis on an SDS-PAGE gel and visualized by autoradiography. (C) Cell surface expression. Cells were collected into PBS containing 0.5 M EDTA at 4.5 h posttransfection, pelleted by centrifugation (1,000 × *g* for 5 min), and fixed with 2% paraformaldehyde. The surface G protein expression was detected with a monoclonal antibody (anti-IE2) to VSIV G, which was subsequently detected by using an anti-mouse IgG secondary antibody conjugated to Alexa Fluor 488. A total of 10,000 cells were counted by flow cytometry. (D) Subcellular localization of G proteins. Epifluorescence images of transfected cells. At 5 h posttransfection cells were fixed and cell surface G was detected by immunostaining with IE2. Where indicated, cells were permeabilized with Triton X-100 to visualize the internal G. Note that G is present throughout the secretory pathway, as expected, and G was transported to the surface in all cases. Experiments were performed three times, and error bars represent the standard deviations.

VSV G, a 65-kDa protein comprising a 20-amino-acid (aa) transmembrane domain and a 29-aa cytoplasmic tail, is cotranslationally inserted in the ER, where the chaperone GRP78 assists in its folding (15). The G monomers associate into noncovalently linked trimers in the ER and are transported to the Golgi complex (47). From the Golgi complex, the trimers are shuttled to the plasma membrane, where viral assembly occurs (46). The trimeric form of G is in a dynamic equilibrium with the monomer throughout the secretory pathway and on the cell surface (46), and it is stabilized by acidic pH (7). The atomic structure of VSV G has been determined in both the pre- and postfusion states (30, 33). G comprises four domains: I (red), II, the trimerization domain (blue), III, the pleckstrin homology (PH) domain (orange), and IV, the fusion domain (yellow) (Fig. 1A). The fusion domain itself consists of two antiparallel β-strands that are linked by the fusion loops. The tips of the loops are hydrophobic and are flanked by charged residues that are proposed to limit the extent of membrane penetration of the loops (30). In the prefusion state G resembles a tripod, where the trimerization domains are in contact but the fusion loops are held away from each other (see Fig. 7A, below). During the transition to the postfusion state, major refolding within the trimerization domain results in the fusion loops moving approximately 160Å. In

the acid pH conformation, the fusion loops are in close proximity with one another and the presumed location of the transmembrane domain (30, 33). Prior to the determination of the structure, mutational analysis identified residues 102 to 123 within the fusion domain as important for fusion (8, 9), but the second hydrophobic loop (W72A, Y73A) had not been shown to play a direct role in fusion. Functional analysis of this second loop has recently confirmed its importance in cell-cell fusion as well as in the infection of retrovirus particles pseudotyped with altered G proteins (39).

In this study, we employed a strategy to produce fully authentic VSV particles that contain lethal mutations in G (20). We elected to do this so that we can examine how authentic viral particles are blocked in assembly or fusion following mutation of the *G* gene and as a means to identify second site suppressors of blocks in viral assembly and fusion. To test our strategy, we initially focused on the hydrophobic tips of the fusion loops. As expected, we found that such mutations abrogate cell-cell fusion and are lethal to infectious VSV. By using a genetic complementation strategy, we amplified such viruses and demonstrated that the mutations in the fusion loops of G do not inhibit protein oligomerization, trafficking to the plasma membrane, or budding of virus particles. Following the repeated passage of those complemented viruses, we identified a single second site suppressor of one such lethal mutation to the fusion loops. The viruses generated in this study provide new tools to mechanistically study how the hydrophobic loops of a class III viral fusogen mediate membrane fusion.

MATERIALS AND METHODS

Cells. BSR-T7 (2) and Vero cells (ATCC) were maintained at 37°C in Dulbecco's modified Eagle's medium (DMEM; Invitrogen, Carlsbad, CA) containing 10% fetal bovine serum (FBS; Tissue Culture Biologicals, Tulare, CA).

Plasmids and site-directed mutagenesis. The VSV *G* gene (NCBI Indiana/Orsay [VSIV], M11048; New Jersey [VSNJV], M27165) was amplified from isolated genomic viral RNA by using one-step reverse transcription-PCR (Qiagen, Germantown, MD) and primers (5′-GCGGTACCATGAAGTGCCTTTTGTACTTAGC-3′ and 5′-GCGGTACCTTACTTTCCAAGTCGGTTCATCTCTATGTC-3′ for VSIV or 5′-GCGGTACCATGTTGTCTTATCTAATCTTTG-3′ and 5′-GCGGTACCCATATATTAACGGAAATGAGCCA-3′ for VSNJV) that contained flanking KpnI sites (underlined). The resulting DNA products were digested with KpnI (New England BioLabs [NEB], Ipswich, MA) and cloned into either pGEM3 (Promega, Madison, WI) or pCAGGS (Belgian Co-ordinated Collections of Microorganisms). Site-directed mutagenesis was performed with complementary oligonucleotides of the following sequence (only sense strand is reported) for W72A, 5′-GTTATATACTCCGGTCCGTACGCGCGGAAATCACAAGTAG-3′, Y73A, 5′-CTTGTGATTTCCGCTGGGCCGGACCGGAGTATATAAC-3′, Y116A, 5′-GCATCCGTCACAGTTGCAGCTCCACAACTTTGAGGAG-3′, A117F, 5′-GCATCCGTCACAGTGTTATATCCACAACTTGAGGAG-3′, and E76K, 5′-CCGCTGGTACGGACCGAAGTATATAACACATTCCATC-3′, using QuikChange mutagenesis (Stratagene, Santa Clara, CA) according to the manufacturer's instructions. All mutations were verified by sequencing the entire *G* gene. To engineer recombinant virus particles, a fragment spanning from the SwaI site to the KpnI site of the mutated *G* gene was transferred into an infectious cDNA clone of VSV that encoded enhanced green fluorescent protein (eGFP), pVSV1+ eGFP (43).

Metabolic labeling of proteins. Confluent monolayers (80%) of BSR-T7 cells in 6-well plates were infected with vaccinia virus expressing T7 polymerase (vTF7-3) (10) at a multiplicity of infection (MOI) of 5. Following 1 h of incubation, cells were washed with phosphate-buffered saline (PBS) and transfected with 0.5 μg DNA/well of pGEM3-VSIV G using Lipofectamine 2000 (Invitrogen). Transfected cells were incubated at 37°C for 5 h and then starved of methionine and cysteine for 1 h. Cells were exposed to 35 μCi of [^{35}S]methionine-cysteine ([^{35}S]Met-Cys) for 2 h and collected as described above. Cytoplasmic extracts were prepared using lysis buffer (1% [vol/vol] NP-40, 0.4% [wt/vol] sodium deoxycholate, 66 mM EDTA, 10 mM Tris-HCl [pH 7.4]) and clarified by centrifugation at 16,000 × *g* for 2 min. Equal amounts of protein as determined by Bradford assay were analyzed by SDS-PAGE and the proteins detected by phosphorimaging analysis (Amersham Bioscience, GE Healthcare, Piscataway, NJ) as previously described (19, 37).

Cell surface expression. BSR-T7 cells at 80% confluence were infected in 35-mm dishes with vTF7-3 at an MOI of 5 and transfected with 0.5 μg of pGEM3-VSIVG by using Lipofectamine 2000 (Invitrogen). Cells were incubated at 37°C for 5 h and collected by scraping into 50 mM EDTA–PBS (137 mM NaCl, 2.682 mM KCl, 8.1 mM Na_2HPO_4, 1.47 mM KH_2PO_4; pH 7.2), followed by centrifugation at 4,000 × *g* for 5 min. Cells were subsequently fixed in 2% paraformaldehyde (PFA) for 20 min, washed several times in PBS, and incubated with a 1:20 dilution of IE2 (VSV G neutralizing antibody [kind gift from Isabel Novella]) (24) in PBS on ice for 30 min. Cells were washed twice in PBS, incubated with a 1:600 dilution of goat anti-mouse Alexa Fluor 488 (Invitrogen) on ice for 30 min, and rinsed in PBS. Following resuspension in 750 μl of 0.5 mM EDTA–PBS, the fluorescence of 10,000 cells from each population was determined by flow cytometry using a FACSCalibur (Becton Dickinson Biosciences, San Jose, CA). The percentage of cells expressing each glycoprotein and the mean fluorescence intensity (MFI) of the transfected population were quantified by flow cytometry. Relative cell surface expression was determined as follows: [(percent cells expressing mutant protein)(MFI mutant population)]/[(percent cells expressing wild-type [wt] protein)(MFI for wt population)].

Indirect immunofluorescence. BSR-T7 cells plated on glass coverslips at 70% confluence were transfected as described for cell surface expression. At 5 h posttransfection, cells were fixed with 2% paraformaldehyde for 15 min and washed twice with PBS, and half of the samples were permeabilized with 0.5% Triton X-100 for 15 min. VSIV G was detected by incubating coverslips with a 1:20 dilution of IE2 for 1 h. Cells were washed twice and incubated with a 1:2,000 dilution of a secondary anti-mouse antibody conjugated to Alexa Fluor 488 (Invitrogen) and a 1:2,000 dilution of 4′,6-diamidino-2-phenylindole (DAPI; Invitrogen). Images were acquired using a Zeiss Axioplan 2 inverted fluorescence microscope (Carl Zeiss MicroImaging, Germany) equipped with a 63× (numerical aperture, 1.4) objective.

Cell-cell fusion assay. BSR-T7 cells at 80% confluence in 96-well plates were infected with vTF7-3 at an MOI of 3 and transfected 1 h later with 0.02 μg DNA/well of pGEM3-VSV G as described above. In parallel, approximately 9 × 10^6 BSR-T7 cells were transfected with pGEM4-FLuc (Promega), which expresses firefly luciferase. At 5 h posttransfection, the pGEM4-FLuc cells were collected as described above, and 50,000 cells were overlaid onto each well of the pGEM3-G-transfected cells. Following a 20-min incubation, the medium was replaced with fusion buffer (10 mM $Na_2HPO_4 \cdot 7H_2O$, 10 mM HEPES, 10 mM morpholineethanesulfonic acid [MES]) of various pH (5.2 to 6.8). The fusion buffer was replaced after 2 min with DMEM containing 2% FBS. Following incubation at 37°C for 1.5 h, the medium was replaced with a 1:1 dilution of Steady Glo (Promega) in PBS, and luciferase values were determined by using a MicroBeta TriLux scintillation counter (Perkin-Elmer, Waltham, MA).

NH_4Cl titration. BSR-T7 cells were seeded in 6-well plates. At 80% confluence, cells were treated with the indicated concentrations of NH_4Cl (EMD Chemicals, Gibbstown, NJ) for 20 min prior to infection. At 5 h postinfection (hpi) cells were collected in 50 mM EDTA–PBS and recovered by centrifugation at 3,000 × *g* for 3 min. The cells were fixed with 2% PFA for 20 min at room temperature, washed twice in PBS, and resuspended in 0.5 mM EDTA–PBS. Levels of eGFP were measured in 10,000 cells by using fluorescence-activated cell sorting (FACS) as described above.

Propagation of lethal mutations. Recombinant VSV particles bearing lethal mutations in the G gene were recovered as described previously (42), except that transfections additionally contained 1.5 μg of pGEM3 New Jersey G. For propagation, 35-mm dishes of approximately 80% confluent BSR-T7 cells were transfected with 1 μg pCAGGS-NJ G and infected 16 h later with the VSIV particles, and cell culture supernatants were collected 24 h later. Virus particles containing only the genome-encoded VSIV G were obtained by performing a final amplification in cells that lacked a complementing G plasmid. The presence of infectious virus was measured using a plaque assay performed as previously described (37).

Endo H sensitivity. Approximately 80% confluent BSR-T7 cells in 6-well plates were infected with New Jersey-complemented VSIV at an approximate MOI of 5. The effective MOI of lethal mutants was determined by measuring the number of eGFP-positive cells after a single round of infection. Following incubation at 37°C for 4.5 h, cells were metabolically labeled by incorporation of 50 μCi of [^{35}S]Met-Cys as above. Following a 10-min labeling period, medium was replaced and supplemented with a 20-fold excess of cold Met-Cys for a variable chase period (15 to 105 min). Cytoplasmic extracts were prepared as described above and treated with 10× endo-β-*N*-acetylglucosaminidase H (endo H) G5

reaction buffer (NEB) and 10× denaturation buffer (NEB) and boiled for 10 min. Half of the sample was subsequently exposed to 40× endo H (NEB) at 37°C for 1 h. Equal quantities of the treated and untreated samples were analyzed by electrophoresis, and G protein was visualized as described above.

Oligomerization assay. Cells were infected with New Jersey-complemented VSIV at an MOI of 10 for 13 h, and proteins were metabolically labeled as above for the endo H assay, except that the labeling period was increased to 20 min followed by a 1.5-h postlabeling chase in the presence of 20-fold Met-Cys. Cell extracts were prepared using 2× MNT (20 mM MES, 30 mM Tris, 100 mM NaCl) plus 1% Triton-X at pH 5.8 to 7 at 37°C for 2 min, clarified by centrifugation at 16,000 × *g* for 2 min, and overlaid on a 5-to-20% continuous sucrose gradient in an SW55Ti rotor (Beckman Coulter, Brea, CA). Following centrifugation at 195,000 × *g* for 15 h, equal fractions were collected from the top of the gradient using a BioLogic LP fractionation system (Bio-Rad, Hercules, CA). The G protein was selectively immunoprecipitated using IE2 at 4°C for 12 h, and complexes were isolated with protein G magnetic beads (NEB). Following three PBS washes, the bound complexes were released by solubilization in loading buffer (200 mM Tris-HCl, 400 mM β-mercaptoethanol, 8% SDS, 40% glycerol) and analyzed by electrophoresis, and G protein was detected as described above.

RESULTS

Mutations to the VSIV G fusion loops are tolerated for protein synthesis and transport. To determine how altering the hydrophobic nature of the fusion loops of VSIV G impacts fusion, the residues in the distal tips of each loop (W72, Y73, and Y116) were individually exchanged for alanine (Fig. 1A). Since an alanine residue (A117) is naturally present in one loop, we exchanged this for phenylalanine. During the course of our study, some of the mutations were shown to block fusion when engineered into the *G* gene of the Mudd-Summers strain of VSIV (39). We generated mutations in the *G* gene from the Orsay strain, and we noticed an important distinction with regard to the effect of the A117F mutation between the two strains. The reason for this distinction is described in detail below.

Substitutions to the VSIV G fusion loops were tolerated for protein expression as measured by metabolic incorporation of [^{35}S]Met-Cys followed by analysis of the proteins by SDS-PAGE (Fig. 1B). To measure cell surface expression of the altered G proteins, we detected the G protein present on the surface of cells by using IE2 and quantified the abundance using flow cytometry. Substitutions W72A (orange), Y73A (yellow), and A117F (blue) were surface expressed at similar levels (85 to 99%) as VSIV G, whereas Y116A (pink) showed a modest but statistically significant reduction to 75% of WT ($P = 0.01$) (Fig. 1C). The reduction in surface expression of Y116A might reflect slower transport kinetics or retention of the protein within the secretory pathway. Despite the modest reduction in surface expression, we did not observe a dramatic retention of Y116A in the endoplasmic reticulum or Golgi complex when the levels of G were examined by indirect immunofluorescence microscopy (Fig. 1D). Taken together, the above experiments revealed that mutation of the fusion loops of VSIV G did not significantly compromise the synthesis or surface expression of mutants in cells.

G loop mutants are defective in cell-cell fusion. To determine whether the altered G proteins mediate membrane fusion, we employed a cell-cell fusion assay. Briefly, BSR-T7 cells expressing T7 RNA polymerase and VSIV G were overlaid with cells containing a plasmid carrying the firefly luciferase gene under the control of a T7 promoter. Exposure of those mixed cells to acidic pH causes the conformational changes in G necessary for membrane fusion, thus mixing the T7 RNA polymerase with the luciferase plasmid, which drives reporter gene expression. Cells expressing wild-type G protein led to a consistent increase in luminescence at pH values below 6.2 (Fig. 2A). By contrast, each substitution to the fusion loops led to a complete inhibition of cell-cell fusion, even at pH 5.2 (Fig. 2A).

Fusion is generally thought to require the concerted refolding of multiple G protein trimers. We reasoned, therefore, that the fusion-defective G proteins would inhibit fusion catalyzed by wild-type G. Transfection of cells with equal quantities of VSIV G and one of the W72A, Y73A, and Y116A mutants resulted in a 50% inhibition of fusion (Fig. 2B). By contrast, A117F diminished fusion by only 25% (Fig. 2B). Increasing the concentration of A117F to a 5:1 ratio compared to the wild type resulted in a 50% inhibition of fusion (Fig. 2C). Theoretically, there are four possible trimer permutations combining the wild type and fusion-defective mutants: all wild type, all mutant, or two mixtures (1 WT:2 MUT and 2 WT:1 MUT). The G proteins of VSIV and share only 70% identity and mixed trimers do not form; thus, we evaluated whether the VSIV G mutants could inhibit VSNJV G fusion (3, 45). Fusion-defective VSIV G did not significantly interfere with membrane fusion catalyzed by VSNJV G, indicating that the inhibition of fusion requires either the formation of mixed trimers or serotype-specific interactions between the trimers themselves (Fig. 2D).

Recombinant vesicular stomatitis virus particles with lethal mutations in the fusion machinery. The above experiments showed that each of the hydrophobic residues of the fusion loops is essential for G-mediated membrane fusion. We sought to determine whether mutations elsewhere in G could compensate for these lethal substitutions. We generated recombinant VSV particles containing the lethal mutations in G and employed a complementation strategy to support their growth, similar to a strategy used to generate viruses with lethal mutations in their membrane-proximal region (20). Briefly, the recovery and propagation of the recombinant VSIV was supported by expression of functional VSNJV G protein in *trans* from a transfected plasmid. To generate virus particles containing only the fusion-defective VSIV G expressed from the viral genome, we performed a final amplification in cells that lack the *trans*-complementing VSNJV G plasmid (Fig. 3A). Using this approach, we recovered virus particles for each mutant and, following amplification and purification, we analyzed their protein composition by SDS-PAGE (Fig. 3B). The overall level of G present in the particles was reduced for recombinants Y73A and Y116A, but W72A and A117F contained similar levels of G as those of preparations of wild-type virus. Viruses were recovered from two independent transfections. Sequence analysis of the viral genomes demonstrated that W72A, Y73A, and Y116A contained the anticipated mutation with no other changes in the *G* gene. By contrast, recombinant A117F contained a single additional coding change in the genome, E76K. This coding change resulted in the ability of the virus particles to grow, since preparations of A117F/E76K formed plaques on Vero cells, in contrast to the particles containing W72A, Y73A, and Y116A G (Fig. 3C). Position 76 is naturally a lysine in the Mudd Summers strain of VSIV, which likely explains why A117F retains fusion activity in that

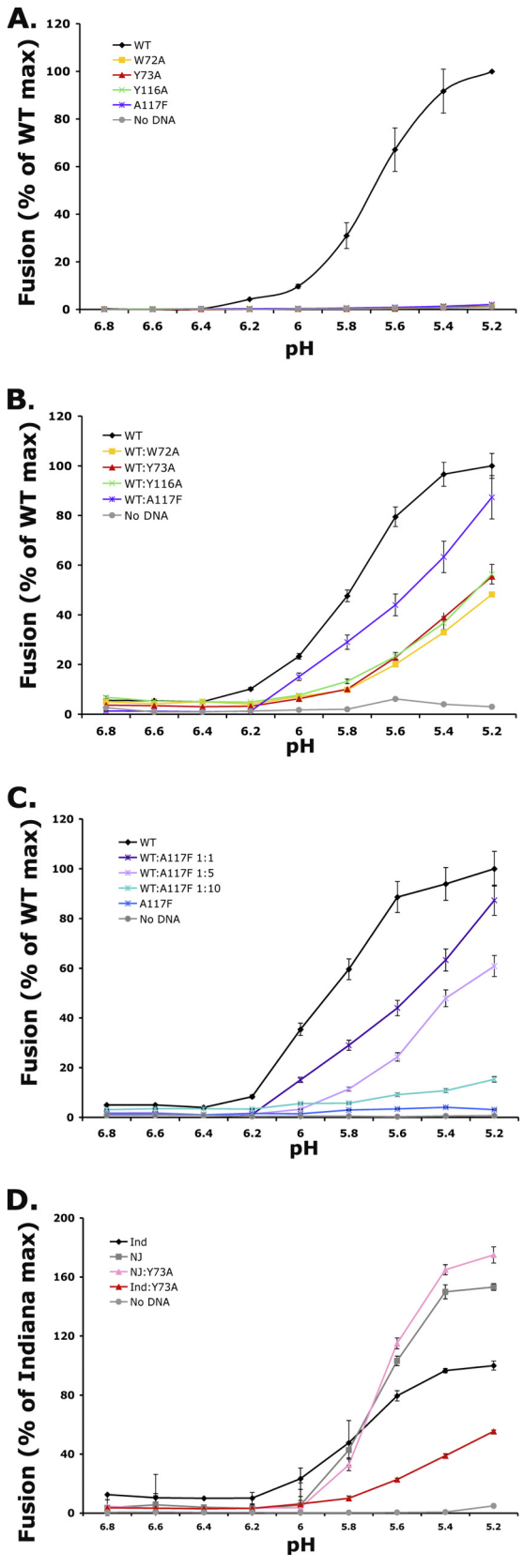

context. These data show that fully assembled authentic VSIV particles bearing lethal mutations in the fusion domain of VSIV G can be generated and that second site suppressor mutations can complement the inhibition of fusion.

The compensatory substitution, E76K, resides in the fusion domain of G and is in close proximity to the first fusion loop comprising W72 and Y73 (see Fig. 7A). This charged residue has been suggested to play a role in mediating the correct positioning of the fusion loop, restricting the depth of membrane insertion (29, 30, 33). To further analyze the properties of this mutant, we evaluated E76K and E76K/A117F in a the cell-cell fusion assay. The substitution E76K catalyzed membrane fusion at more neutral pH than the wild type, with fusion clearly detected at pH 6.4. When E76K and A117F were combined, fusion was less efficient than for E76K but still occurred at a more neutral pH than for VSIV G (Fig. 4A). This suggests that the E76K mutation may function to destabilize the G protein, resulting in a lower proton concentration required for fusion. To test this idea, we evaluated whether viruses containing the E76K substitution were less sensitive to inhibition by ammonium chloride (NH_4Cl), which neutralizes the acidic environment of endosomes and lysosomes. Recombinant viruses containing simply the E76K mutation or with the double mutation E76K/A117F were less sensitive to NH_4Cl inhibition of infection compared to wild-type virus (Fig. 4B). This decreased sensitivity of viral infection to ammonium chloride extends the cell-cell fusion results and supports the idea that viruses containing the E76K substitution fuse at a pH of >6.2.

Effects of lethal mutations in the VSIV G fusion domain on G transport and oligomerization. Although assessment of surface expression of each of the G mutants indicated that there was no major inhibition of cell surface expression following mutation of the fusion domain, those experiments did not determine whether the kinetics of G transport were altered. To examine the kinetics of G transport, we employed an endo H sensitivity assay (34). Endo H cleaves high-mannose structures found on proteins prior to their transit to the medial Golgi apparatus, and further modification of those glycans in the *trans*-Golgi complex results in endo H resistance (35). This allows determination of the rate and movement of the G proteins in the secretory pathway. We infected cells with the recombinant particles at an equivalent MOI of 5 and labeled

FIG. 2. Cell-cell fusion assay. BSR-T7 cells in 96-well plates were infected with vTF7-3 at an MOI of 3 and transfected with 0.02 μg/well of VSIV G. At 5 h posttransfection, the VSIV G-expressing cells were overlaid with cells containing a luciferase plasmid, which requires T7 RNA polymerase for expression. Low-pH fusion buffer was added to cells for 2 min to allow for conformational changes in G, thereby producing fusion. Cells were allowed to recover for 1 h, and luciferase levels were analyzed with a luminometer. (A) Wild-type and altered VSIV G proteins were expressed independently; however, only wild-type G was capable of promoting cell-cell fusion. (B) Wild-type VSIV G was combined with an equal molar ratio of fusion-defective VSIV G proteins. Expression of fusion-defective proteins along with the wild type poisons the wild-type fusion reaction. (C) Wild-type VSIV G was combined with various molar ratios of A117F. (D) VSNJV G protein was expressed in equal molar ratios with VSIV fusion-defective proteins. Only Y73A is shown, but W72A, Y116A, and A117F behaved similarly. All experiments were performed four times, and error bars represent the standard deviations between experiments.

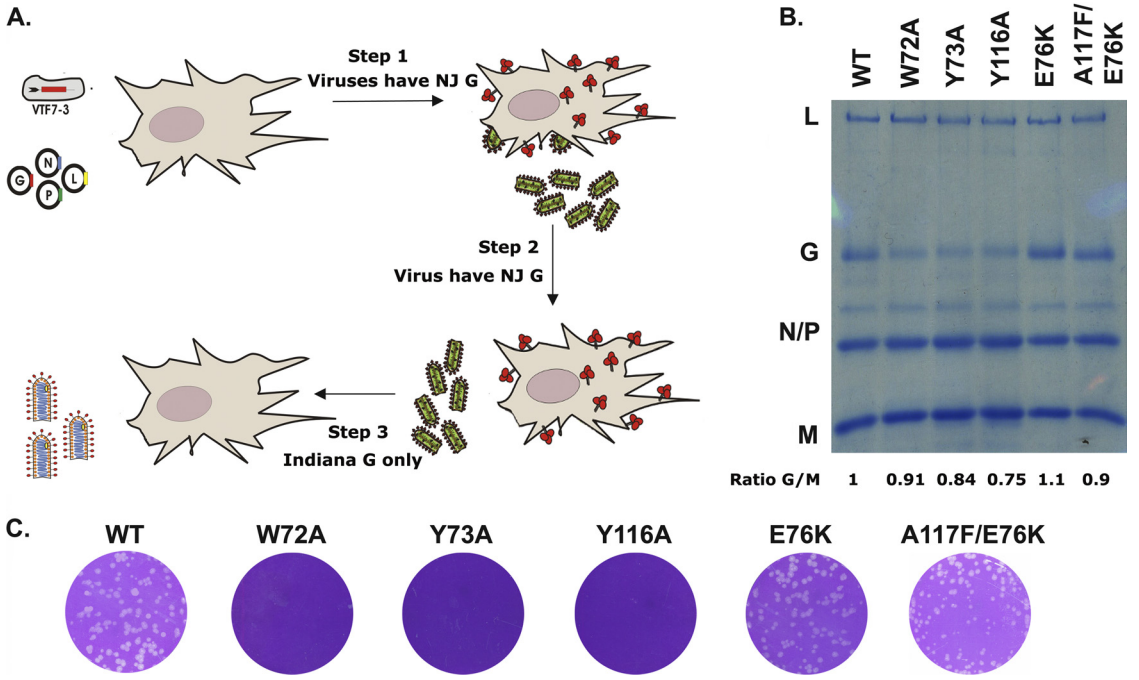

FIG. 3. Lethal virus production. (A) Schematic for the method for producing viruses harboring fusion-defective G proteins. Step 1, recombinant viruses were produced using the previously established method (42); however, a New Jersey G protein (shown in red) was included to complement the fusion-defective phenotype of the viruses. Step 2, viruses containing lethal mutations were passaged in cells expressing New Jersey G protein. Step 3, viruses which only expressed the altered G protein were produced, with a final round of amplification in the absence of New Jersey G. (B) A Coomassie-stained 10% low-bis SDS-PAGE gel of equal amounts of wild-type and altered VSIV G viruses. L, G, N, P, and M refer to the five viral proteins. The G/M ratio was determined and is an average of three experiments. (C) Plaque assays of samples shown in panel B. The assayed plaques were incubated for 24 h at 37°C.

proteins by metabolic incorporation with a pulse of [^{35}S]Met-Cys at 4.5 hpi. Following a variable chase period with unlabeled methionine and cysteine, cytoplasmic extracts were exposed to endo H prior to SDS-PAGE (Fig. 5A and B). This analysis showed that the kinetics of Y116A transport were modestly slowed compared with wild-type G and that W72A, Y73A, E76K, and A117F/E76K were essentially indistinguishable from the wild type (Fig. 5C). This delayed transport may account for the slightly reduced surface expression of Y116A compared to wild-type G (Fig. 1C).

In the ER, G associates into trimers prior to transport to the cell surface. During this transit, the trimers can exchange monomers, although the trimeric form is stabilized by acidic pH (7). To examine whether there were differences in the oligomerization of the G mutants, we infected cells with the recombinant particles as above and monitored the oligomeric state of G. Briefly, cells were infected and exposed to [^{35}S]Met-Cys as described above, and cytoplasmic extracts were sedimented through a 5-to-20% continuous sucrose gradient at different pHs. Gradient fractions were analyzed by SDS-PAGE to determine the oligomerization status of G (Fig. 6). As expected, wild-type G was found mostly in oligomeric forms (bottom of gradient) at pHs of $<$6.2 but was found as a monomer and an oligomer at pHs of $>$6.4. Recombinants W72A, Y73A, and Y116A showed a higher proportion of monomeric G throughout the pH range examined, although oligomeric G increased in abundance at pH 5.8 and 6.0, respectively. This suggests that the oligomers are less stable than those formed by wild-type G. Recombinants E76K and E76K/A117F were more similar to wild-type G, with a shift to more oligomeric G at pH 6.4, respectively. This is consistent with the pH $>$6.2 threshold of cell-cell fusion for E76K. Collectively, these studies show that recombinants bearing lethal mutations in G can be used to effectively study the oligomerization and transport of G, and they show that some mutations to the fusion loops (Y116A) can slow the kinetics of transport of G. Furthermore, this work shows that the substitutions to the fusion loops reduce the stability of G protein oligomers, which might impact their ability to mediate fusion.

DISCUSSION

In this study we determined the consequences for viral entry and assembly following the introduction of lethal mutations in the fusion loops of VSV G. One lethal mutation, designed to increase the hydrophobicity of one of the two fusion loops (A117F), led to the identification of a second site suppressor mutation, E76K, which we speculate helps position the fusion loops in a way that permits their insertion into the lipid bilayer. In addition to understanding the role of the fusion loops of VSIV G, our work shows authentic recombinant VSIV particles that bear lethal mutations in G. Such mutants should serve as excellent tools to probe steps of virus-cell fusion, and we further demonstrated that this approach can be exploited to study viral assembly. Finally, this study has implications for

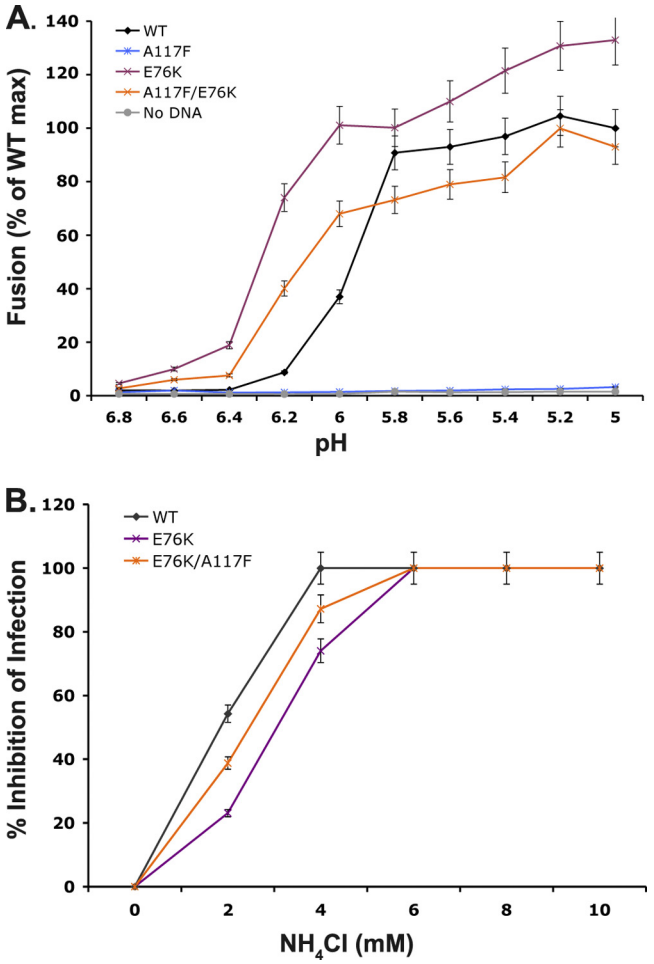

FIG. 4. Effect of an observed compensatory mutation on cell-cell fusion of the mutant A117F. (A) A cell-cell fusion assay (previously described for Fig. 2) was used to determine the effect of the E76K mutation. The single E76K mutation was able to mediate fusion at a pH of >6.2. A117F is unable to mediate cell-cell fusion on its own; however, when combined with E76K it regains fusion activity with a pH profile similar to E76K. (B) Titration of sensitivity to NH_4Cl. Cells were pretreated with NH_4Cl at the indicated concentrations, and eGFP-expressing viruses were allowed to infect in the presence of NH_4Cl. The neutralization was maintained throughout the infection, and at 5 hpi eGFP expression was monitored via FACS analysis. The wild type is more sensitive to this neutralization than viruses that contain the E76K mutation in G. All experiments were performed in triplicate; error bars indicate standard deviations.

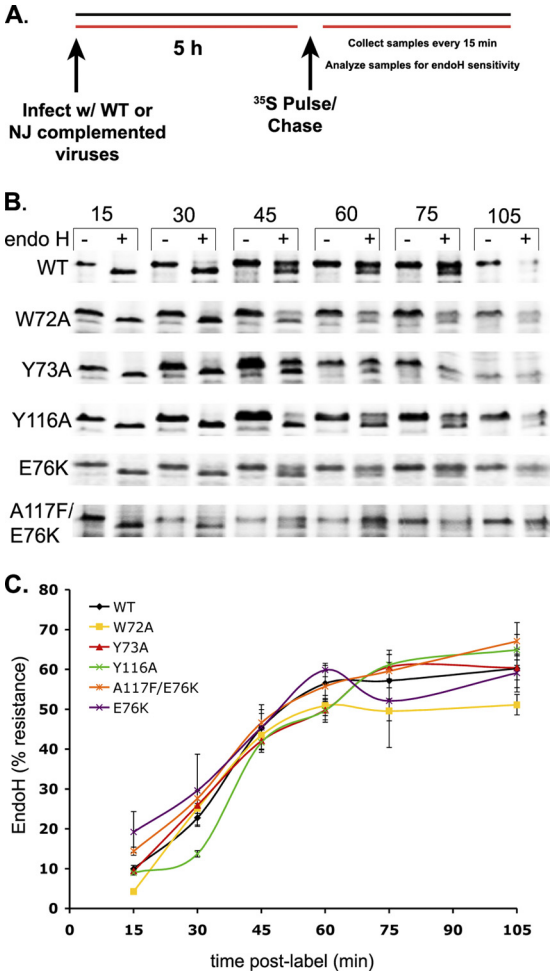

FIG. 5. Endo H sensitivity assay. BSR-T7 cells were infected at an MOI of 5 with viruses containing either wild-type or altered G proteins. Cells were exposed to [^{35}S]Met-Cys for 10 min, and, after the indicated chase period were examined for endo H sensitivity as described in Materials and Methods. (A) Diagram of the experimental protocol. (B) SDS-PAGE gels showing the expressed G proteins and their sensitivities to endo H. (C) Quantification of results shown in panel B. All experiments were performed in triplicate; error bars represent the standard deviations.

strategies to dominantly interfere with the fusion mechanism of VSV G and perhaps other class III fusogens.

The hydrophobic fusion loops of VSIV G are essential for cell-cell fusion but not G oligomerization or transport. This study extends previous work that established that the hydrophobic nature of the fusion loops of VSIV G were important for membrane fusion (39). Specifically, in the present study we harnessed the power of viral genetics to uncover the importance of altering the hydrophobicity of the fusion loops of VSV G. In prior experiments, substitutions to positions W72, Y73, Y116, and A117 were evaluated for their ability to mediate low pH-triggered cell-cell fusion, as well as their ability to mediate infection of pseudotyped MLV particles (39). Parallel to the findings here, the previous work found that substitutions W72A, Y73A, and Y116A were unable to mediate cell-cell fusion. In contrast to that earlier study, where A117F resulted in 50% fusion activity in a cell-cell fusion assay, in our hands this substitution was inactive for cell-cell fusion. The reason for this difference is explained by the identification of E76K as a second site suppressor mutation of A117F. While substitutions W72A, Y73A, and Y116A failed to generate infectious virus particles, A117F produced infectious recombinant VSIV particles that contained a single additional substitution, E76K. Amino acid 76 is naturally a lysine in the Mudd Summers strain of VSIV, which was used in the earlier study, explaining the distinction between our findings (39). We verified that our initial starting clone contained a glutamic acid residue at position 76, and we showed that lysine is always present in the recovered virus. Since we do not observe this mutation in other

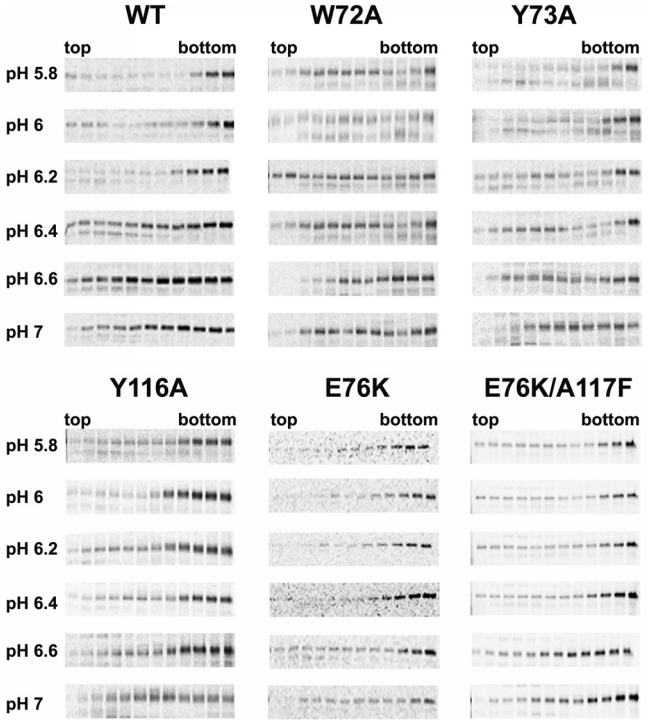

FIG. 6. Oligomerization assay. BSR-T7 cells were infected at an MOI of 10 with viruses containing wild-type or altered G proteins. Cells were exposed to [^{35}S]Met-Cys for 20 min and after the chase period were centrifuged over a sucrose gradient and examined for their trimerization as described in Materials and Methods. Wild-type G was found in the heavier fractions (bottom) of the gradient for fractions at a pH of ≤6.2, where its conformational change takes place. Above pH 6.2, wild-type G was found in both monomeric and oligomeric fractions. W72A, Y73A, and Y116A look similar to the wild type except their transition occurs at pH 6.0. A117F/E76K and E76K show a transition at a more neutral pH, between 6.6 and 6.4, similar to their cell-cell fusion profile.

recovered viruses, including the wild type, this mutation appears to be a bona fide suppressor of the A117F substitution.

The compensatory effect of this mutation was also supported by data obtained in a cell-cell fusion assay. Here, A117F was fusion incompetent, but in combination with E76K efficient fusion occurred. When E76K was examined in the context of the parental G sequence, fusion was more efficient at lower proton concentrations (pH 6.4 versus 6.2). This suggests that E76K alone destabilizes the prefusion conformer of G and may facilitate the conformational changes that drive membrane fusion. Although we cannot be certain about precisely how the A117F mutation blocks membrane fusion, or how E76K compensates for this block, examination of the locations of E76K and A117F in the pre- and postfusion structures offer some insights (Fig. 7). In the prefusion structure, the hydrophobic loops point away from one another, but in the postfusion structure all six fusion loops are in close proximity. One possibility is that the presence of a fourth hydrophobic residue may promote interactions between the loops themselves rather than with the target membrane, and thus impede fusion. Notably, across all members of the *Rhabdoviridae* family, there are never more than three hydrophobic residues at the tips of the loops. In the model shown, the hydrophobic residues are angled away from one another, owing to a steric hindrance following addition of A117F (Fig. 7). Perhaps the second site mutation, E76K, helps position the fusion loops so that the hydrophobic residues can still insert into the target cell membrane, avoiding this steric hindrance.

The atomic structures of the pre- and postfusion forms of G offer some insight into how the pH transition between the two forms is controlled. The current model suggests that a set of histidine residues H60, H162, and H407 comprise a pH-sensitive switch. As the virus encounters acidic pH, those residues become protonated and facilitate the transition to the postfusion conformation. The postfusion conformation of G is stabilized by a network of hydrogen bonding interactions that include D268, D274, E276, D393, and D395, which are either solvent exposed in the prefusion state or inaccessible. Amino acids D137, Y139, H407, and P408 cluster together in the postfusion conformation and stabilize the trimerization domain. It is less clear, however, how the substitution E76K alters the pH of fusion, since this residue seems unlikely to directly influence the residues involved in stabilizing either the pre- or postfusion forms.

The importance of the hydrophobic loops in class III viral fusogens has also been shown for HSV gB and baculovirus gp64. For gB, the hydrophobic residues are surrounded by charged residues which are thought to help position the loops to interact with the polar heads of the lipid bilayer (16, 17). Mutations of hydrophobic and polar residues of gp64 fusion loops abolish syncytium formation (22). In the case of gp64 the pretransmembrane domain, which is adjacent to the fusion loops, appears to interact with the fusion loops (25). Although the pretransmembrane domain of VSIV G was not resolved in the atomic structure (30, 33), one intriguing possibility is that substitution E76K could perhaps promote repulsion between the fusion domain and pretransmembrane domain and that this also destabilizes the fusion protein.

Although the mechanism by which E76K compensates for the additional hydrophobic residue within the adjacent fusion loop is not clear, our results show that lack of cell-cell fusion is not due to protein expression, oligomerization, or transport (Fig. 1B and C and 6). In fact, we found that all fusion-incompetent mutants were able to reach the cell surface, although Y116A was transported slightly slower than wild type (Fig. 5). We noticed, however, that the stability of the oligomers formed by the various G mutants was altered and that this correlated with the inability to mediate fusion. Mutants W72A, Y73A, and Y116A did not form oligomers as stable as wild type or the E76K mutants (Fig. 6). How altering the hydrophobicity of the fusion loops results in this alteration to the stability of G oligomers is not certain, but this observation underscores that mutations in the fusion loops can impact a step of viral assembly. This reduced stability may account for the apparent reduction in the level of G protein present on the surface of those purified virus particles (Fig. 3B).

Is there a cooperative mechanism for G mediated fusion? Cell-cell fusion was blocked by substitutions in the fusion loops, and those substitutions interfered with the capacity of VSIV but not VSNJV G to mediate fusion. There are two possible explanations for this serotype-specific inhibition of fusion. The fusion-incompetent G could form mixed trimers with the VSIV G and thus poison fusion, as has been shown

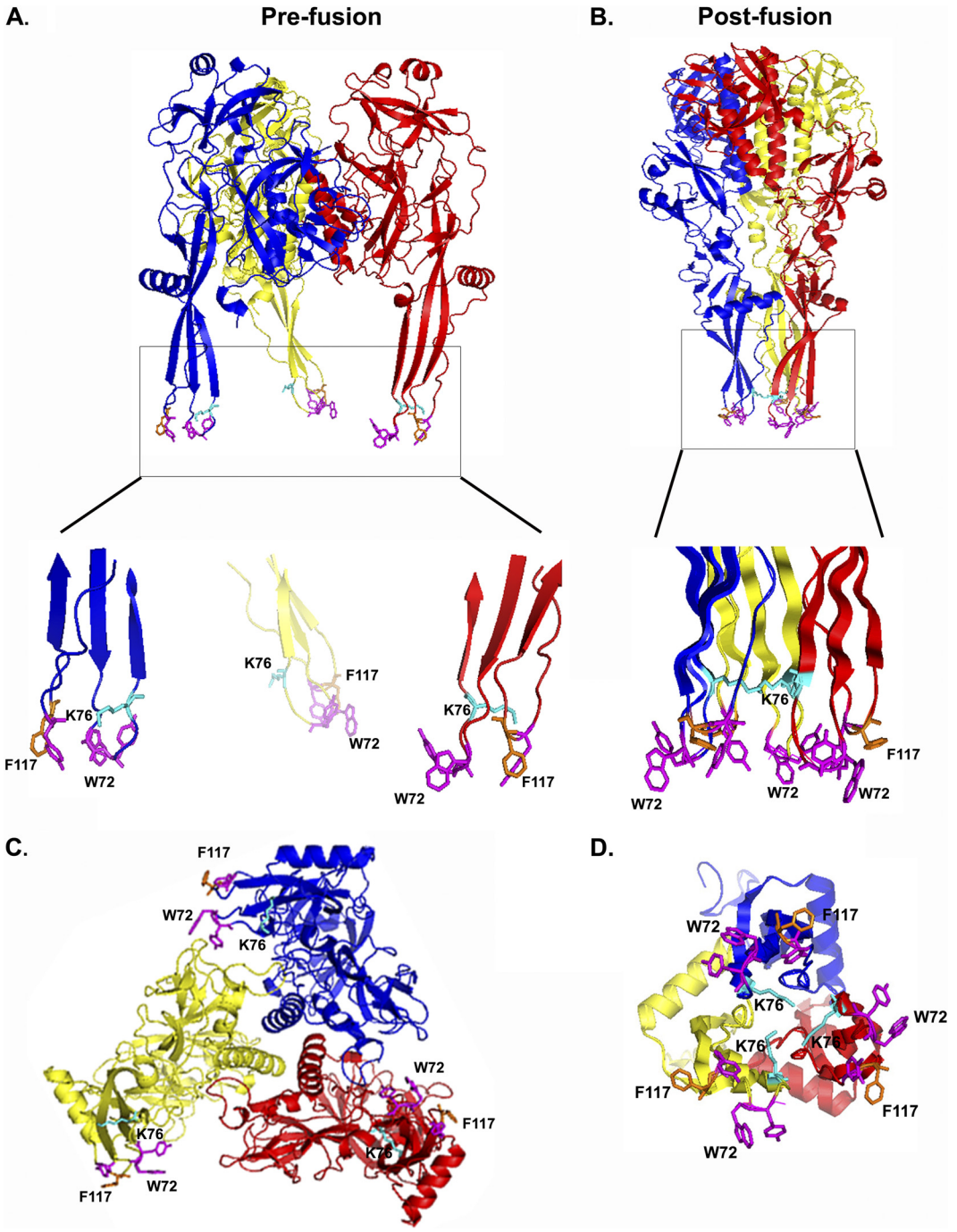

FIG. 7. Structure of VSIV G, showing the impact of substitutions E76K and A117F. The least-disruptive rotamer conformation of each glycoprotein mutation was modeled according to the VSIV G prefusion structure electron density map (PDB accession number 2J6J) using the software Coot (7a). The hydrophobic tips containing W72, Y73, and Y116 are shown in magenta, residue F117 is orange, and K76 is shown in cyan. A close-up of the fusion loops and the intratrimer interactions are shown in prefusion (A) and postfusion (B) conformations. Views of the intratrimer interactions are shown in prefusion (C) and postfusion (D) conformations.

previously for other fusion-incompetent mutants (45). Since G protein can exchange between trimer and monomer at the cell surface (46), such a mechanism for inhibition seems plausible. An additional explanation is that intertrimer interactions that are posited to facilitate fusion (26) may depend upon physical serotype-specific interactions between the trimers themselves. The spikes of G protein visible by electron microscopic analysis of viral particles form a hexameric lattice on the surface of the virion following exposure of the particles to acidic pH, consistent with the possibility of intertrimer interactions.

The ability of the different fusion-defective G proteins to block membrane fusion is also distinct. Specifically, A117F

requires a 5-fold-higher concentration than W72A, Y73A, or Y116A to yield a 50% inhibition of wild-type fusion (compare Fig. 2B and C). There are four different trimer combinations possible (3 WT; 3 MUT; 1 WT:2 MUT; 2 WT:1 MUT). The difference in the ability of each mutant to poison the wild-type reaction may reflect the fact that W72A, Y73A, and Y116A in all three combinations (3 MUT, 1 WT:2 MUT, or 2 WT:1 MUT) can poison fusion; however, for A117F, mixed trimers containing 1 or 2 molecules of A117F may themselves be functional for fusion. This would suggest that the A117F poisoning of fusion may require intertrimer interactions. For rabies virus, it has been suggested that the refolding of as many as 16 trimers are required to drive membrane fusion (11, 12, 32). If a similarly high threshold is required for VSIV G, this may necessitate a significant number of A117F homotrimers to poison wild-type fusion. Although such cooperativity may not require interactions among the trimers themselves, defects in the oligomerization status of the fusion loop mutants may impact this cooperativity such that the energy derived from refolding of G is insufficient to complete the fusion process.

Genetic stability of viruses containing lethal mutations in G. The mutations in G themselves appear to have distinct genetic stabilities. Specifically, following 16 passages, W72A, Y73A, and Y116A all retained the original mutation. By contrast, the mutation E76K was by P1 selected for and fixed within the A117F population. The differential ability of A117F to interfere with wild-type fusion offers an explanation as to why this specific mutation led to the generation of a second site suppressor. Once the E76K mutation arises in the virus population, very high concentrations of A117F would be required to block the fusion mediated by E76K; consequently, the E76K mutation is quickly selected for within the population. By contrast, since similar amounts of W72A, Y73A, and Y116A block wild-type fusion, it seems likely that the large excess of these proteins produced in cells will dominantly interfere with small amounts of fusion-competent proteins generated during viral growth, perhaps accounting for the difficulty in isolating second site suppressors of these mutations. This differential dominant inhibition of membrane fusion mediated by the different mutations in the fusion loops of VSV G has potential impacts for strategies to target fusion to block infection. The selection of escape mutants to A117F occurs readily, whereas despite 16 passages of the W72, Y73, and Y116 substitutions, we failed to identify any second site suppressors of the fusion loop mutations. This argues that direct targeting of the hydrophobic tips of the fusion loops themselves is much more likely to be an effective antiviral strategy than drugs blocking fusion by targeting the surrounding regions. Screens for fusion inhibitors that simply report on fusion are likely to result in a range of compounds that include molecules that target both the fusion loops themselves and the surrounding sequences. While each class of molecule will block fusion, the likelihood of selecting resistance mutations is profoundly distinct. Our work therefore also identifies dominant targets within the glycoprotein of VSV that may be shared among the class III fusogens.

Utility of viruses containing lethal mutations in G. An important goal of this study was to generate authentic recombinant VSV particles bearing lethal mutations. We chose the residues in the fusion loops as a model to develop this method. We showed that we can produce Coomassie-stainable quantities of viruses bearing lethal mutations in G. Although lethal mutations in G could be studied using existing pseudotyping approaches (14, 39), the system described here offers several advantages. Those advantages include the higher efficiency of incorporation of G into the authentic particle and the ability to harness the power of forward genetics to isolate compensatory mutations in G. Although the properties of both the A117F substitution and the E76K compensatory mutation can be studied in the context of viral pseudotypes or cell-cell fusion assays, the identification of E76K as a bona fide compensatory change would likely have proved considerably more difficult if using a pseudotyping approach.

This study provides a panel of lethal mutations in G that can be used to probe the mechanism of membrane fusion as well as study the requirements for G transport and assembly. It will be of interest to now use these virus particles to probe at what step of fusion the various mutants are blocked and possibly to determine the site of membrane fusion within the cell.

ACKNOWLEDGMENTS

This study was supported by NIH grant AI081842 to S.P.J.W. S.P.J.W. is a Burroughs Wellcome Fund Investigator in the Pathogenesis of Infectious Disease. M.L.S. is supported by NIH Ruth Kirschstein award F32 AI089052.

We thank John Chorba for his contributions to a progenitor of this study in showing that A117F blocks cell-cell fusion and Philip Kranzusch for his assistance in modeling the subsitutions.

REFERENCES

1. **Bloor, S., J. Maelfait, R. Krumbach, R. Beyaert, and F. Randow.** 2010. Endoplasmic reticulum chaperone gp96 is essential for infection with vesicular stomatitis virus. Proc. Natl. Acad. Sci. U. S. A. **107:**6970–6975.
2. **Buchholz, U. J., S. Finke, and K. K. Conzelmann.** 1999. Generation of bovine respiratory syncytial virus (BRSV) from cDNA: BRSV NS2 is not essential for virus replication in tissue culture, and the human RSV leader region acts as a functional BRSV genome promoter. J. Virol. **73:**251–259.
3. **Bussereau, F., and A. Flamand.** 1978. Coinfection with a rhabdovirus: vesicular stomatitis virus of Indiana and New Jersey serotypes. Ann. Microbiol. (Paris) **129B:**71–86.
4. **Carneiro, F. A., A. S. Ferradosa, and A. T. Da Poian.** 2001. Low pH-induced conformational changes in vesicular stomatitis virus glycoprotein involve dramatic structure reorganization. J. Biol. Chem. **276:**62–67.
5. **Coil, D. A., and A. D. Miller.** 2004. Phosphatidylserine is not the cell surface receptor for vesicular stomatitis virus. J. Virol. **78:**10920–10926.
6. **Cureton, D. K., R. H. Massol, S. Saffarian, T. L. Kirchhausen, and S. P. Whelan.** 2009. Vesicular stomatitis virus enters cells through vesicles incompletely coated with clathrin that depend upon actin for internalization. PLoS Pathog. **5:**e1000394.
7. **Doms, R. W., et al.** 1988. Differential effects of mutations in three domains on folding, quaternary structure, and intracellular transport of vesicular stomatitis virus G protein. J. Cell Biol. **107:**89–99.

7a. **Emsley, P., B. Lohkamp, W. G. Scott, and K. Cowtan.** 2010. Features and development of Coot. Acta Crystallogr. D Biol. Crystallogr. **66:**486–501.

8. **Fredericksen, B. L., and M. A. Whitt.** 1996. Mutations at two conserved acidic amino acids in the glycoprotein of vesicular stomatitis virus affect pH-dependent conformational changes and reduce the pH threshold for membrane fusion. Virology **217:**49–57.
9. **Fredericksen, B. L., and M. A. Whitt.** 1995. Vesicular stomatitis virus glycoprotein mutations that affect membrane fusion activity and abolish virus infectivity. J. Virol. **69:**1435–1443.
10. **Fuerst, T. R., E. G. Niles, F. W. Studier, and B. Moss.** 1986. Eukaryotic transient-expression system based on recombinant vaccinia virus that synthesizes bacteriophage T7 RNA polymerase. Proc. Natl. Acad. Sci. U. S. A. **83:**8122–8126.
11. **Gaudin, Y., R. W. Ruigrok, M. Knossow, and A. Flamand.** 1993. Low-pH conformational changes of rabies virus glycoprotein and their role in membrane fusion. J. Virol. **67:**1365–1372.
12. **Gaudin, Y., et al.** 1999. Rabies virus-induced membrane fusion. Mol. Membr. Biol. **16:**21–31.
13. **Gaudin, Y., C. Tuffereau, D. Segretain, M. Knossow, and A. Flamand.** 1991. Reversible conformational changes and fusion activity of rabies virus glycoprotein. J. Virol. **65:**4853–4859.
14. **Ge, J., et al.** 2006. Generating vesicular stomatitis virus pseudotype bearing

the severe acute respiratory syndrome coronavirus spike envelope glycoprotein for rapid and safe neutralization test or cell-entry assay. Ann. N. Y. Acad. Sci. **1081:**246–248.
15. **Hammond, C., and A. Helenius.** 1994. Folding of VSV G protein: sequential interaction with BiP and calnexin. Science **266:**456–458.
16. **Hannah, B. P., et al.** 2009. Herpes simplex virus glycoprotein B associates with target membranes via its fusion loops. J. Virol. **83:**6825–6836.
17. **Hannah, B. P., E. E. Heldwein, F. C. Bender, G. H. Cohen, and R. J. Eisenberg.** 2007. Mutational evidence of internal fusion loops in herpes simplex virus glycoprotein B. J. Virol. **81:**4858–4865.
18. **Harrison, S. C.** 2008. Viral membrane fusion. Nat. Struct. Mol. Biol. **15:**690–698.
19. **Heinrich, B. S., D. K. Cureton, A. A. Rahmeh, and S. P. Whelan.** 2010. Protein expression redirects vesicular stomatitis virus RNA synthesis to cytoplasmic inclusions. PLoS Pathog. **6:**e1000958.
20. **Jeetendra, E., et al.** 2003. The membrane-proximal region of vesicular stomatitis virus glycoprotein G ectodomain is critical for fusion and virus infectivity. J. Virol. **77:**12807–12818.
21. **Johannsdottir, H. K., R. Mancini, J. Kartenbeck, L. Amato, and A. Helenius.** 2009. Host cell factors and functions involved in vesicular stomatitis virus entry. J. Virol. **83:**440–453.
22. **Kadlec, J., S. Loureiro, N. G. Abrescia, D. I. Stuart, and I. M. Jones.** 2008. The postfusion structure of baculovirus gp64 supports a unified view of viral fusion machines. Nat. Struct. Mol. Biol. **15:**1024–1030.
23. **Le Blanc, I., et al.** 2005. Endosome-to-cytosol transport of viral nucleocapsids. Nat. Cell Biol. **7:**653–664.
24. **Lefrancios, L., and D. S. Lyles.** 1982. The interaction of antiody with the major surface glycoprotein of vesicular stomatitis virus. I. Analysis of neutralizing epitopes with monoclonal antibodies. Virology **121:**157–167.
25. **Li, Z., and G. W. Blissard.** 2009. The Autographa californica multicapsid nucleopolyhedrovirus GP64 protein: analysis of transmembrane domain length and sequence requirements. J. Virol. **83:**4447–4461.
26. **Libersou, S., et al.** 2010. Distinct structural rearrangements of the VSV glycoprotein drive membrane fusion. J. Cell Biol. **191:**199–210.
27. **Matlin, K. S., H. Reggio, A. Helenius, and K. Simons.** 1982. Pathway of vesicular stomatitis virus entry leading to infection. J. Mol. Biol. **156:**609–631.
28. **Mire, C. E., J. M. White, and M. A. Whitt.** 2010. A spatio-temporal analysis of matrix protein and nucleocapsid trafficking during vesicular stomatitis virus uncoating. PLoS Pathog. **6:**e1000994.
29. **Roche, S., A. A. Albertini, J. Lepault, S. Bressanelli, and Y. Gaudin.** 2008. Structures of vesicular stomatitis virus glycoprotein: membrane fusion revisited. Cell Mol. Life Sci. **65:**1716–1728.
30. **Roche, S., S. Bressanelli, F. A. Rey, and Y. Gaudin.** 2006. Crystal structure of the low-pH form of the vesicular stomatitis virus glycoprotein G. Science **313:**187–191.
31. **Roche, S., and Y. Gaudin.** 2002. Characterization of the equilibrium between the native and fusion-inactive conformation of rabies virus glycoprotein indicates that the fusion complex is made of several trimers. Virology **297:**128–135.
32. **Roche, S., and Y. Gaudin.** 2004. Evidence that rabies virus forms different kinds of fusion machines with different pH thresholds for fusion. J. Virol. **78:**8746–8752.
33. **Roche, S., F. A. Rey, Y. Gaudin, and S. Bressanelli.** 2007. Structure of the prefusion form of the vesicular stomatitis virus glycoprotein G. Science **315:**843–848.
34. **Rose, J. K., and J. E. Bergmann.** 1983. Altered cytoplasmic domains affect intracellular transport of the vesicular stomatitis virus glycoprotein. Cell **34:**513–524.
35. **Rothman, J. E., and H. F. Lodish.** 1977. Synchronised transmembrane insertion and glycosylation of a nascent membrane protein. Nature **269:**775–780.
36. **Schlegel, R., T. S. Tralka, M. C. Willingham, and I. Pastan.** 1983. Inhibition of VSV binding and infectivity by phosphatidylserine: is phosphatidylserine a VSV-binding site? Cell **32:**639–646.
37. **Schott, D. H., D. K. Cureton, S. P. Whelan, and C. P. Hunter.** 2005. An antiviral role for the RNA interference machinery in Caenorhabditis elegans. Proc. Natl. Acad. Sci. U. S. A. **102:**18420–18424.
38. **Sieczkarski, S. B., and G. R. Whittaker.** 2003. Differential requirements of Rab5 and Rab7 for endocytosis of influenza and other enveloped viruses. Traffic **4:**333–343.
39. **Sun, X., S. Belouzard, and G. R. Whittaker.** 2008. Molecular architecture of the bipartite fusion loops of vesicular stomatitis virus glycoprotein G, a class III viral fusion protein. J. Biol. Chem. **283:**6418–6427.
40. **Sun, X., V. K. Yau, B. J. Briggs, and G. R. Whittaker.** 2005. Role of clathrin-mediated endocytosis during vesicular stomatitis virus entry into host cells. Virology **338:**53–60.
41. **Thomas, D., et al.** 1985. Mass and molecular composition of vesicular stomatitis virus: a scanning transmission electron microscopy analysis. J. Virol. **54:**598–607.
42. **Whelan, S. P., L. A. Ball, J. N. Barr, and G. T. Wertz.** 1995. Efficient recovery of infectious vesicular stomatitis virus entirely from cDNA clones. Proc. Natl. Acad. Sci. U. S. A. **92:**8388–8392.
43. **Whelan, S. P., J. N. Barr, and G. W. Wertz.** 2000. Identification of a minimal size requirement for termination of vesicular stomatitis virus mRNA: implications for the mechanism of transcription. J. Virol. **74:**8268–8276.
44. **White, J., K. Matlin, and A. Helenius.** 1981. Cell fusion by Semliki Forest, influenza, and vesicular stomatitis viruses. J. Cell Biol. **89:**674–679.
45. **Whitt, M. A., P. Zagouras, B. Crise, and J. K. Rose.** 1990. A fusion-defective mutant of the vesicular stomatitis virus glycoprotein. J. Virol. **64:**4907–4913.
46. **Zagouras, P., and J. K. Rose.** 1993. Dynamic equilibrium between vesicular stomatitis virus glycoprotein monomers and trimers in the Golgi and at the cell surface. J. Virol. **67:**7533–7538.
47. **Zagouras, P., A. Ruusala, and J. K. Rose.** 1991. Dissociation and reassociation of oligomeric viral glycoprotein subunits in the endoplasmic reticulum. J. Virol. **65:**1976–1984.